Advances in Applied Mathematics and Mechanics
Adv. Appl. Math. Mech., Vol. **2**, No. 4, pp. 467-482

DOI: 10.4208/aamm.10-m1008
August 2010

Lattice Boltzmann Modeling of Viscous Elementary Flows

Mohammed A. Boraey[1,*] and Marcelo Epstein[1]

[1] *Mechanical and Manufacturing Engineering Department, University of Calgary, 2500 University Drive NW, Calgary, Alberta, T2N 1N4, Canada*

Received 11 February 2010; Accepted (in revised version) 20 April 2010

Available online 28 May 2010

Abstract. A lattice Boltzmann method is developed for modeling viscous elementary flows. An adjustable source term is added to the lattice Boltzmann equation, which can be tuned to model different elementary flow features like a doublet or a point source of any strength, including a negative source (sink). The added source term is dimensionally consistent with the lattice Boltzmann equation. The proposed model has many practical applications, as it can be used in the framework of the potential flow theory of viscous and viscoelastic fluids. The model can be easily extended to the three dimensional case. The model is verified by comparing its results with the analytical solution for some benchmark problems. The results are in good agreement with the analytical solution of the potential flow theory.

AMS subject classifications: 76D06, 76M28, 82D15

Key words: The Lattice Boltzmann method, Chapman-Enskog expansion, source term, point source, point sink, doublet, viscous elementary flows, potential flow theory, symmetry.

1 Introduction

The development of the lattice Boltzmann method (LBM) has rapidly grown in the last two decades. The reason for this; is the easiness of use of the technique in addition to its ability to solve a variety of problems that are impractical or even impossible to be solved by traditional computational fluid dynamics (CFD) techniques.

Since its appearance, many researchers have tried to make the method more powerful by modifying its equations to incorporate more physical phenomena. Examples of this include the lattice Boltzmann method for axisymmetric fluid flow [3], axisymmetric thermal flows [22], multiphase flow [14] and viscous fingering phenomenon [1].

The potential flow theory has always been thought of as a theory for irrational inviscid flow problems. However, a lot of recent literature investigated the potential

*Corresponding author.
Email: maboraey@ucalgary.ca (M. A. Boraey), mepstein@ucalgary.ca (M. Epstein)

use of the potential flow theory for viscous and viscoelastic fluids at low Reynolds numbers [5, 17–19].

Thus, modeling of the elementary flow features using the lattice Boltzmann method adds new capabilities to the technique and opens new frontiers for its potential use.

Several researchers have tried to solve fluid flow problems involving different types of singularities. In the case of geometrical singularities, [9] has introduced a series solution for the steady flow of a viscous fluid in the neighbourhood of a sharp corner. [4] have proposed a method to incorporate this series solution into a finite difference scheme for the solution of the stream function/vorticity formulation of the Navier-Stokes equations in the case of a rectangular re-entrant corner. The scheme is successful in overcoming the singularity problem of the velocity gradient near a sharp corner. They have used their proposed scheme to solve the flow field in a channel with a sudden contraction.

For cases where stress singularities arise from abrupt changes in boundary conditions in viscous flow problem, [2] proposed a singular finite element scheme for stokes flow and used it to solve for the flow field of the stick-slip problem. They have used special elements surrounding the singular point without a pressure node at the singular point. They showed that ordinary finite element schemes are less accurate in the neighbourhood of the singular point. The scheme is also useful for high Reynolds number flows and for Non-Newtonian fluids provided that the stresses are integrable.

The reference [7] proposed a moving mesh finite element algorithm for problems in two and three space dimensions. Their scheme is successful in solving various problems (including fluid dynamics problems) with regions of high gradients.

In this paper, an easy-to-implement and efficient way of modeling elementary flows through the incorporation of a point source, sink and a doublet using the lattice Boltzmann method is proposed for the first time. The results of the numerical simulations are compared to the analytical solution of the potential flow theory and are in excellent agreement.

Modeling elementary flow features has always been a challenge for numerical modeling. The reason is the associated mathematical singularity at the point of interest. To the best of the authors' knowledge, numerical methods based on the solution of the continuum conservation equations like finite difference and finite element have never been used to model a point source, sink or doublet using a single point in the computational domain.

Due to the continuum approach considerations, only one value for each variable can be assigned at a certain point at a specific time instant. For example, at any point only one value for the macroscopic flow velocity can be specified or calculated. However, due to the nature of the lattice Boltzmann method formulation and the fact that it does not deal directly with the macroscopic variables, the local distribution function can be formulated in such a way to allow for different proportions of particles to move along different directions, see Fig. 1. Then, these microscopic velocities stream to neighbour lattices' nodes during the streaming step. This allows for the modeling of a point source through a single lattice node.

From a practical point of view, modeling a point source is a necessity when dealing with physical problems in which the dimension of the source is much less than that of the domain. In this case the best practice is to model this source as a point source.

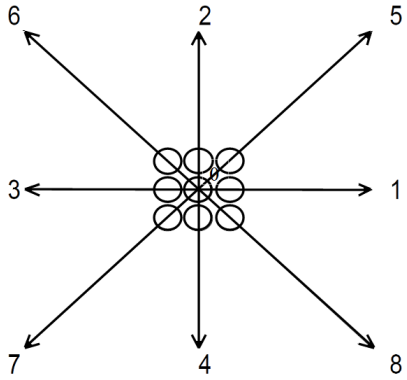

Figure 1: The lattice velocities of the D2Q9 lattice (Adopted from [20]).

Modeling a doublet with the lattice Boltzmann method has many potential applications, the most important of which is the modeling of flow around circular cylinders by adding a uniform velocity field to the doublet. The doublet strength can be tuned to produce a circular cylinder of a certain diameter. This approach has the advantage of modeling the flow around the exact circular geometry which overcomes the disadvantages of using approximate Cartesian geometries generated by square lattices or the need for a special treatment for curved boundaries [8] which greatly complicates the computations.

2 The Lattice Boltzmann equation

The proposed model is based on the standard lattice Boltzmann equation which can be written as [23]

$$f_i(\mathbf{X} + \mathbf{e_i}\Delta t, t + \Delta t) - f_i(\mathbf{X}, t) = \Omega, \tag{2.1}$$

where f_i is the particles distribution function, $\mathbf{X} = (x, y)$ is the position vector, $\mathbf{e_i}$ is the lattice speed along the i^{th} direction, Δt is the time step and Ω is the collision operator.

In the present study, the two dimensional nine-speed D2Q9 lattice configuration is adopted, see Fig. 1. For which $\mathbf{e_i}$ is defined as [21]

$$\mathbf{e_i} = \begin{cases} (0,0)e, & i = 0, \\ (\pm 1, 0)e, (0, \pm 1)e, & i = 1, 2, 3, 4, \\ (\pm 1, \pm 1)e, & i = 5, 6, 7, 8, \end{cases} \tag{2.2}$$

where $e = \Delta x/\Delta t$ and Δx is the lattice size.

The collision operator Ω can be approximated by the BGK (Bhatnagar, Gross and Krook) model as in [15]:

$$\Omega = \omega(f_i^{eq} - f_i) = \frac{1}{\tau}(f_i^{eq} - f_i), \tag{2.3}$$

where $\omega = 1/\tau$ is the relaxation frequency, τ is a single relaxation time and f^{eq} is the local equilibrium distribution function.

Substituting the collision operator Ω defined by (2.3) into (2.1) yields the lattice Boltzmann equation for the BGK collision model as

$$f_i(\mathbf{X} + \mathbf{e_i}\Delta t, t + \Delta t) - f_i(\mathbf{X}, t) = \frac{1}{\tau}(f_i^{eq} - f_i). \tag{2.4}$$

The local equilibrium distribution function f^{eq} for the D2Q9 lattice configuration is given by [16]

$$f_i^{eq}(\mathbf{X}) = \omega_i \rho(\mathbf{X})\Big(1 + \frac{3\mathbf{e_i}\cdot\mathbf{U}}{e^2} + \frac{9}{2}\frac{(\mathbf{e_i}\cdot\mathbf{U})^2}{e^4} - \frac{3}{2}\frac{\mathbf{U^2}}{e^2}\Big), \tag{2.5}$$

where

$$e = 1, \qquad \text{i.e.,} \quad \Delta x = \Delta t, \tag{2.6a}$$

$$\omega_i = \begin{cases} 4/9, & i = 0, \\ 1/9, & i = 1,2,3,4, \\ 1/36, & i = 5,6,7,8. \end{cases} \tag{2.6b}$$

ρ is the macroscopic fluid density defined as

$$\rho = \sum_{i=0}^{8} f_i = \sum_{i=0}^{8} f_i^{eq}, \tag{2.7}$$

$\mathbf{U}$ is the macroscopic fluid velocity defined as

$$\mathbf{U}_j = \frac{1}{\rho}\sum_{i=0}^{8} f_i \mathbf{e}_{ij} = \frac{1}{\rho}\sum_{i=0}^{8} f_i^{eq}\mathbf{e}_{ij}, \tag{2.8}$$

where $\mathbf{e}_{ij}$ is the j component of the lattice speed along the i direction. The pressure p is defined as

$$p = c_s^2 \rho, \tag{2.9}$$

where c_s is the speed of sound for the LB scheme. For the D2Q9 model, $c_s = 1/\sqrt{3}$.

The kinematic ν viscosity is given by [21]

$$\nu = \Big(\tau - \frac{1}{2}\Big)c_s^2 \Delta t. \tag{2.10}$$

3 The Lattice Boltzmann equation for elementary flows

From a physical point of view, in order to model a point source or sink a pressure difference has to be generated between the point of interest and the surrounding points in all directions. This pressure difference will drive the flow outward or inward to mimic a point source or sink respectively. The added source term mainly consists of a reference density ρ_s weighted by a weighting factor Φ_i. Since the pressure and density in the lattice Boltzmann method are related by the equation of state, this term is analogous to a pressure term. The generated pressure difference is determined by the value of the reference density ρ_s; while the weighting factor Φ_i ensures that this pressure difference is the same in all directions.

The proposed lattice Boltzmann equation for modeling a point source, sink or doublet can be written as

$$f_i(\mathbf{X}+\mathbf{e_i}\Delta t, t+\Delta t) - f_i(\mathbf{X}, t) = \frac{1}{\tau}(f_i^{eq} - f_i) + \Delta t \Gamma \Phi_i \rho_s, \tag{3.1}$$

where the added source term is $\Delta t \Gamma \Phi_i \rho_s$, in which ρ_s is a reference density; Φ_i is a weighting factor for ρ_s; Γ is the source, sink or doublet strength.

The meaning and values of these parameters are given in details in the following sections.

3.1 The source term reference density ρ_s

The reference density ρ_s is the density upon which the source, sink or doublet strength will be based.

There are three ways to specify the reference density ρ_s. The best way is determined by the application at hand. It is important to mention here that having more than one way to specify the reference density ρ_s, gives more flexibility to model different physical situations.

3.1.1 Case I

The first way is to set ρ_s equal to the local density ρ at the point of interest. In this case the strength will be a function of the fluid local density and may change during the course of unsteady flow simulations. This way the reference density ρ_s is given by

$$\rho_s = \rho. \tag{3.2}$$

Specifying the reference density ρ_s this way ensures the generation of a point source or sink at the point of interest regardless of the local flow conditions at this point. However, the pressure difference and the resulting pressure at the point of interest will not be known ahead. This case is suitable for physical situations in which the source or/and sink strength is/are only dependent on the local flow conditions.

3.1.2 Case II

The second way is to set ρ_s equal to a constant value ρ_o which is pre-specified. In this case the strength will be constant regardless of the flow conditions. However; the flow conditions will affect the effective fluid density at the point of interest through f^{eq}. In this case the reference density ρ_s is given by

$$\rho_s = \rho_o. \tag{3.3}$$

In this case, the source or/and sink strength is/are constant. In other words, the pressure difference between the point of interest and the surrounding points is constant. This is suitable for situations in which a constant pressure difference is required during the course of simulation regardless of the local flow conditions. However, the pressure at the point of interest will not be constant and will depend in-part on the fluid local density.

3.1.3 Case III

The third way is to set ρ_s in such a way that ensures a constant reference density ρ_c regardless of the fluid local density. This is done by eliminating the effect of the fluid local density introduced by f^{eq}.

The reference density ρ_s is given by

$$\rho_s = \rho_c - \frac{\rho}{\tau\,\Delta t\Gamma}, \qquad \text{for a point source,} \tag{3.4a}$$

$$\rho_s = -\rho_c + \frac{\rho}{\tau\,\Delta t\Gamma}, \qquad \text{for a point sink.} \tag{3.4b}$$

In this case, the $(\rho/\tau\Delta t\Gamma)$ cancels the effect of the first term of f^{eq} (Eq. (2.5)), which represents the fluid local density and results in a constant density of ρ_c at the point of interest.

Case III is suitable for situations in which a constant value of the pressure at the point of interest is required. In this case this value will be constant during the simulation regardless of the flow conditions. But the resulting pressure difference between the point of interest and the surrounding points will depend on the flow conditions. A good example of this is in oil wells simulations, which maintains a constant suction pressure at the production well that does not depend on the oil pressure inside the reservoir.

The value of ρ_c should be selected very carefully if the nature of the point of interest is required to stay the same. The selection of the reference density ρ_s in this way

Table 1: Pressure and pressure difference at the point of interest for different cases of specifying the reference density ρ_s.

	Case I	Case II	Case III
Pressure	Varies	Varies	Constant
Pressure Difference	Varies	Constant	Varies

completely cancels the effect of the flow conditions on the pressure at the point of interest. For example, in the case of a point source, ρ_c should have a value that is always greater than the fluid density of the surrounding points. If during the simulation, especially for unsteady cases, the density of the surrounding points drops below ρ_c, the point of interest will act as a sink instead of acting as a source. The same is true in case of a point sink. Table 1 summarizes the features of each case regarding the pressure.

The formulation of the source term in this way has the advantage of using the point source/sink or doublet at any point inside the domain or on a symmetry plane without any adjustments to the strength Γ or the reference density ρ_s.

3.2 The reference density weighting factor Φ_i

Φ_i is the weighting factor for the reference density ρ_s. Its value depends on the nature of the point of interest. For example, the value of Φ_i, in case of a point source, ensures that the increase in the pressure at the source point is the same with respect to all neighbour points.

The values of Φ_i for a normal point and for a point with a source or sink are given by

$$\Phi_i = \begin{cases} 0, & \text{any point,} \\ w_i, & \text{source,} \\ -w_i, & \text{sink.} \end{cases} \tag{3.5}$$

It is clear that the weighting factor for the point source or sink posses point symmetry. This allows the point source to be located on any symmetry plane passing through the lattice center ($i = 0$) without the need for a special treatment. The source term has zero net momentum so it conserves the lattice momentum.

For a doublet, the value of Φ_i is given by

$$\Phi_i = \begin{cases} 0, & i = 0, 2, 4, \\ w_i, & i = 3, 6, 7, \\ -w_i, & i = 1, 5, 8. \end{cases} \tag{3.6}$$

The weighting factor for the doublet posses line symmetry around the line passing through the lattice center ($i = 0$) and parallel to the lattice directions ($i = 1$ or 3).

3.3 The strength parameter Γ

The strength Γ is a positive number that determines how far the source, sink or doublet strength will depend on the reference density ρ_s. The strength can be a multiple (or a fraction) of the reference density ρ_s.

The value of Γ should be chosen according to the physics of the problem. Γ is the only parameter that controls the strength in Case I. For Cases II and III, ρ_o and ρ_c also contribute to the strength respectively.

Very small values for Γ will not cause any stability problems (as in the case of a doublet and flow around a circular cylinder that will be shown in the results section).

However, large unphysical values for Γ (and ρ_o or ρ_c) will affect the solution stability. From Eq. (3.1), it can be shown that large values for Γ in case of a point source can cause flow reversal at some points in the domain (i.e., inflow boundary) and in case of a point sink can cause negative values for the particle distribution function.

3.4 Derivation of the continuum equivalent of the proposed LB equation

In order to recover the macroscopic continuum equivalent of the proposed LB equation, the Chapman-Enskog expansion [6] is performed.

The proposed LB equation is given by Eq. (3.1). Assuming Δt is small and is equal to ε, i.e.,

$$\Delta t = \varepsilon, \tag{3.7}$$

then Eq. (3.1) can be written as

$$f_i\left(\mathbf{X}+\mathbf{e_i}\varepsilon, t+\varepsilon\right) - f_i(\mathbf{X}, t) = \frac{1}{\tau}(f_i^{eq} - f_i) + \varepsilon\Gamma\Phi_i\rho_s, \tag{3.8}$$

taking the Taylor series expansion of the left-hand side of this equation for a small change ε in time leads to

$$\varepsilon\Big(\frac{\partial}{\partial t} + \mathbf{e}_{ij}\frac{\partial}{\partial x_j}\Big)f_i + \frac{1}{2}\varepsilon^2\Big(\frac{\partial}{\partial t} + \mathbf{e}_{ij}\frac{\partial}{\partial x_j}\Big)^2 f_i + \mathcal{O}(\varepsilon^3) = \frac{1}{\tau}(f_i^{eq} - f_i) + \varepsilon\Gamma\Phi_i\rho_s, \tag{3.9}$$

the particle distribution function f_i can be expanded as following [24]

$$f_i = f_i^{(0)} + \varepsilon f_i^{(1)} + \varepsilon^2 f_i^{(2)} + \mathcal{O}(\varepsilon^3), \tag{3.10}$$

with the following constraints [12]

$$\sum_i f_i^{(0)} = \rho, \qquad \sum_i f_i^{(0)}\mathbf{e}_{ij} = \rho\mathbf{U}_j, \tag{3.11a}$$

$$\sum_i f_i^{(n)} = 0, \qquad \sum_i f_i^{(n)}\mathbf{e}_{ij} = 0, \quad n > 0. \tag{3.11b}$$

Eq. (3.9) to the order ε^0 is given by

$$f_i^{(0)} = f_i^{eq}, \tag{3.12}$$

and to the order ε^1 is given by

$$\varepsilon\Big(\frac{\partial}{\partial t} + \mathbf{e}_{ij}\frac{\partial}{\partial x_j}\Big)f_i^{(0)} = \frac{1}{\tau}\Big(f_i^{eq} - f_i^{(0)} - \varepsilon f_i^{(1)}\Big) + \varepsilon\Gamma\Phi_i\rho_s. \tag{3.13}$$

Substitution of Eq. (3.12) into Eq. (3.13) yields

$$\varepsilon\Big(\frac{\partial}{\partial t} + \mathbf{e}_{ij}\frac{\partial}{\partial x_j}\Big)f_i^{(0)} = \frac{1}{\tau}\Big(f_i^{(0)} - f_i^{(0)} - \varepsilon f_i^{(1)}\Big) + \varepsilon\Gamma\Phi_i\rho_s, \tag{3.14a}$$

$$\Big(\frac{\partial}{\partial t} + \mathbf{e}_{ij}\frac{\partial}{\partial x_j}\Big)f_i^{(0)} = \frac{1}{\tau}f_i^{(1)} + \Gamma\Phi_i\rho_s, \tag{3.14b}$$

summation of Eq. (3.14b) over i yields

$$\frac{\partial}{\partial t}\Big(\sum_i f_i^{(0)}\Big) + \frac{\partial}{\partial x_j}\Big(\sum_i \mathbf{e}_{ij} f_i^{(0)}\Big) = \sum_i \Gamma \Phi_i \rho_s, \tag{3.15}$$

substitution of Eqs. (2.8), (2.9) and (3.12) into Eq. (3.15) yields

$$\frac{\partial \rho}{\partial t} + \frac{\partial(\rho \mathbf{u}_j)}{\partial x_j} = \alpha \Gamma \rho_s. \tag{3.16}$$

This is the mass conservation equation with the source term $\alpha\Gamma\rho_s$. α is calculated from Eqs. (3.5) and (3.6) and is given by

$$\alpha = \sum_i \Phi_i = \begin{cases} 1, & \text{source,} \\ -1, & \text{sink,} \\ 0, & \text{doublet.} \end{cases} \tag{3.17}$$

This derivation of the conservation of mass equation from the proposed LB equation ensures that the proposed equation can accurately model various elementary flow features and is capable of recovering the macroscopic equivalent of them.

4 Numerical results

Results of numerical simulations for several cases using the proposed lattice Boltzmann equation are presented and compared to the results from the potential flow theory. Although the use of the proposed equation is general and not limited to these cases, they were selected as they represent benchmark problems for modeling elementary flows and the analytical solutions for them are available [11, 13].

It is important to mention that in some cases there is a small difference between the LBM solution and the analytical solution of the potential flow theory. This difference is due to two facts. The first one is that the LBM models a real fluid with a finite viscosity while the potential flow theory deals with a hypothetical inviscid flow. The second is due to the effect of the boundary conditions which are necessary for the LBM simulation (and for any numerical method) while it does not exist in the case of the potential flow solution. Several boundary conditions were examined in order to minimize their effect on the solution.

Table 2 shows various boundary conditions used during simulations. In the table, open boundary condition refers to Zero gradient of the distribution function normal to the boundary [23]. Velocity boundary condition refers to velocity inlet boundary conditions as proposed by [25].

Symmetry boundary conditions [10] are used in some cases for the top and bottom boundaries. They tend to make the streamlines parallel to the boundary. Open boundary condition was found to be the best choice to minimize the boundary effects. In some cases like the Rankine Oval and the Circular cylinder, the results for the symmetry and open boundary conditions for the top and bottom boundaries are almost

Table 2: Boundary conditions for different simulation cases.

	Left boundary (Inflow)	Top and bottom boundaries	Right boundary (outflow)
Source, Sink	Open	Open	Open
Doublet	Symmetry	Symmetry	Symmetry
Rankine-Half body	Velocity	Open	Open
Rankine Oval	Velocity	Symmetry/Open	Open
Circular cylinder	Velocity	Symmetry/Open	Open

identical. It is only in the case of a doublet that the symmetry boundary condition gives the best result.

To minimize the effect of the boundary conditions on the simulation results, the domain size in each direction in the simulation is two-times that of the corresponding potential flow. Results are presented for the central part of the domain away from the boundaries to be consistent with the potential flow simulations.

The number of grid points for the potential flow calculations is 200×200, while it is 400×400 for the lattice Boltzmann simulations. For all simulations, the initial conditions are a zero velocity field with a density of unity. The relaxation time τ and the time step Δt were set to unity for all simulations.

All the results are plotted in terms of the normalized stream function, so that the results of LBM and the analytical solution may be compared directly.

4.1 Point source or sink

A point source/sink is a point inside the domain from which the flow is flowing radially outward/inward in all directions. A point source and sink are modeled with the proposed equation (Eq. (3.1)) and the results are compared to the analytical solution of the potential flow theory. For both cases the strength Γ was set to 0.3 based on $\rho_s = \rho$ (Case I).

Fig. 2 shows the normalized radial velocity profile for both cases compared to the analytical solution. As shown in the figure results are in good agreement. It is worth

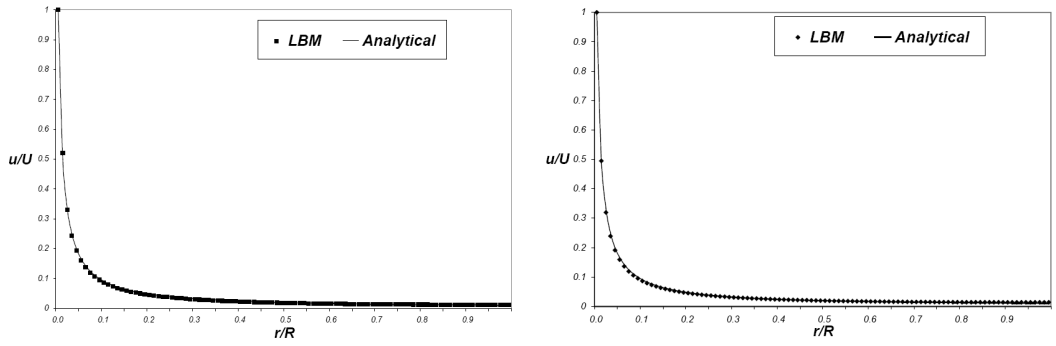

Figure 2: Normalized radial velocity profile: Point source (left), Point Sink (right).

mentioning that the velocity at the point source or sink, for the LBM simulation is finite which overcomes the disadvantage of infinite value in the case of the potential flow solution.

4.2 Rankine-Half body

The Rankine-Half body is formed, when a uniform velocity flow field is combined with a point source. In this case the free stream velocity u_{lattice} is set to 0.001 and the source strength Γ is 0.2 based on $\rho_s = \rho$ (Case I).

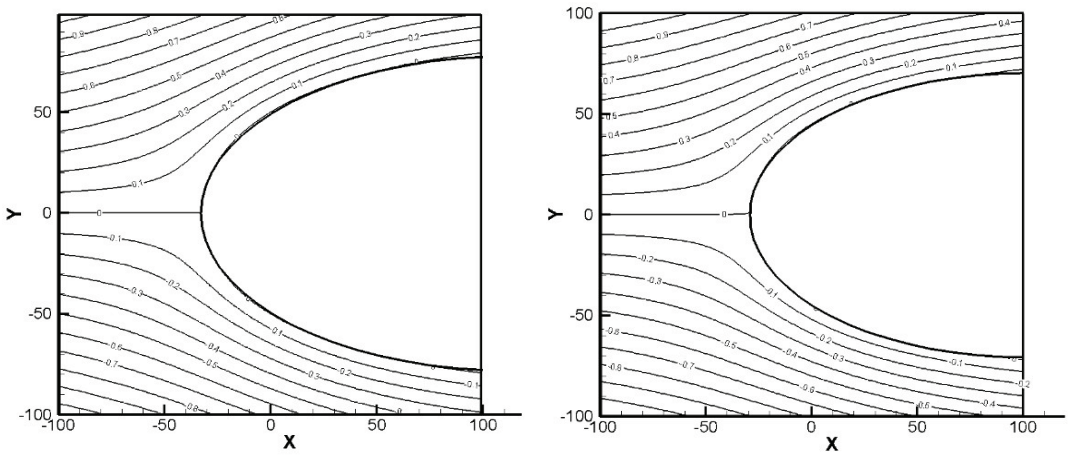

Figure 3: Normalized stream function contours for the Rankine-Half Body: LBM (left), Analytical (right).

Fig. 3 shows the normalized stream function contours for the Rankine-half body from the LBM simulation (left) and the analytical solution of the potential flow theory (right).

In order to demonstrate the ability of the proposed equation to handle different physical situations, the Rankine-Half body is reproduced for Case II and III.

4.2.1 Case I

From the simulation results of the Rankine-Half Body for Case I, ρ was found to be 1.08 which is a reasonable value for a flow starting from an initial condition of zero velocity, density equal to one and inlet velocity of 0.001.

In order to reproduce the same solution for Cases II and III, we need to achieve the same fluid local density ρ at the point of interest.

4.2.2 Case II

Writing Eq. (3.1) for Cases I and II results in the following value of the reference density for Case II

$$\rho_s = \rho_o = 1.08. \tag{4.1}$$

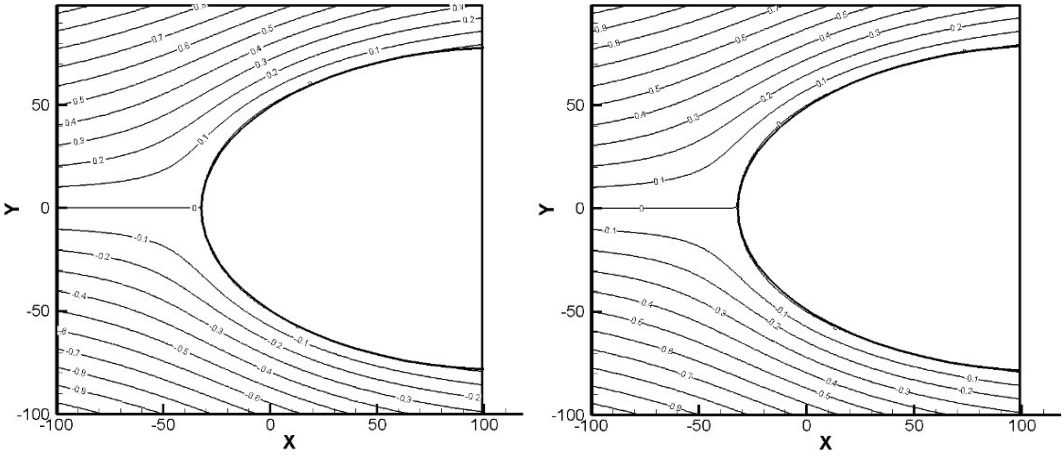

Figure 4: Normalized stream function contours for the Rankine-Half Body by LBM: Case II (left), Case III (right).

Fig. 4 (left) shows the normalized stream function contours for the Rankine-Half body. In this case the free stream velocity u_{lattice} is set to 0.001 and the source strength Γ is 0.2 based on $\rho_s = 1.08$ (Case II).

4.2.3 Case III

Writing Eq. (3.1) for Cases I and III results in the following value of the reference density for Case III

$$\rho_c = \Big(\frac{1}{\Delta t \tau \Gamma} + 1\Big)\rho. \tag{4.2}$$

If we use the same value of Γ for both Cases ($\Gamma = 0.2$), we get ρ_c as

$$\rho_c = \Big(\frac{1}{0.2} + 1\Big)1.08 = 6.48, \tag{4.3}$$

so the reference density ρ_s is given by

$$\rho_s = 6.48 - \frac{\rho}{\Gamma}. \tag{4.4}$$

Fig. 4 (right) shows the normalized stream function contours for the Rankine-Half body. In this case the free stream velocity u_{lattice} is set to 0.001 and the source strength Γ is 0.2 based on $\rho_s = 6.48 - \rho/\Gamma$ (Case III).

Through an analysis similar to the one given above, the equivalent reference density ρ_s can be calculated for different cases.

4.3 Rankine oval

Rankine Oval is formed by combining a uniform velocity field of $u_{\text{lattice}} = 0.001$ with a point source and point sink of strength $\Gamma = 0.1$ based on $\rho_s = \rho$ (Case I) placed 40 lattice units apart along the x-direction.

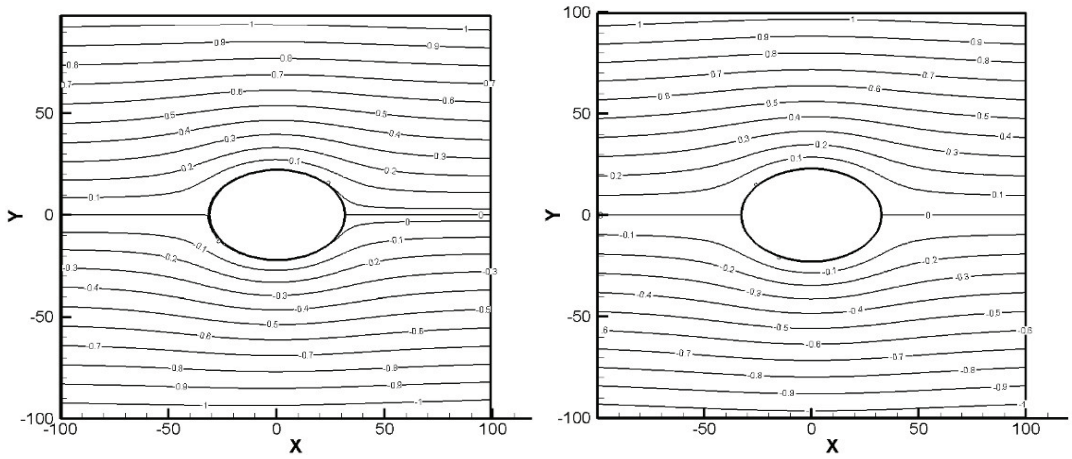

Figure 5: Normalized stream function contours for the Rankine Oval: LBM (left), Analytical (right).

The comparison of the normalized stream function contours in Fig. 5 shows a very good agreement with the results obtained from the potential flow theory.

4.4 Doublet

A doublet is modeled using the proposed equation (Eq. (3.1)). The doublet strength Γ is 0.005 based on $\rho_s = \rho$ (Case I). Fig. 6 shows the normalized stream function contours for the doublet using LBM and the analytical solution of the potential flow theory. As can be seen from the figure there are two main differences between the LBM simulation and the analytical solution.

The normalized stream function contours in the case of the LBM solution are not circular as in the case of the potential flow. Also, contours of different values do not

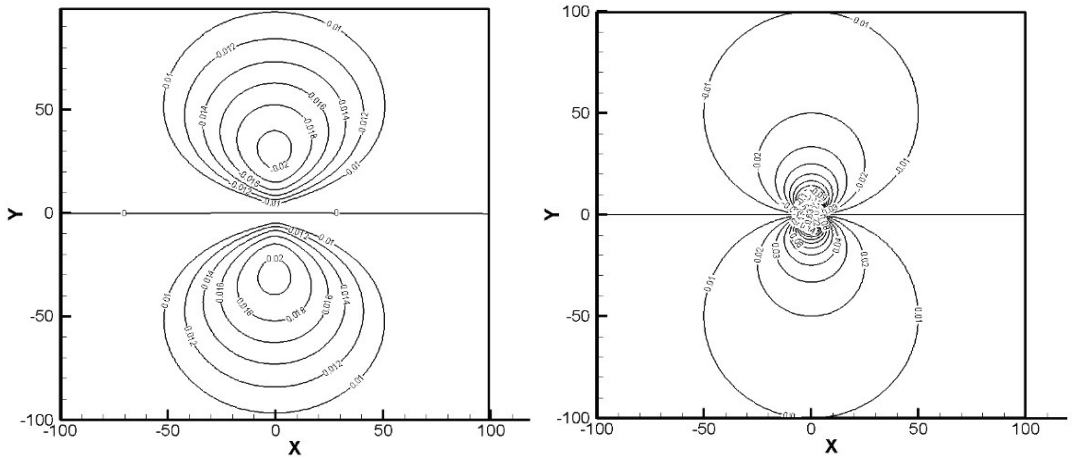

Figure 6: Normalized stream function contours for the Doublet: LBM (left), Analytical (right).

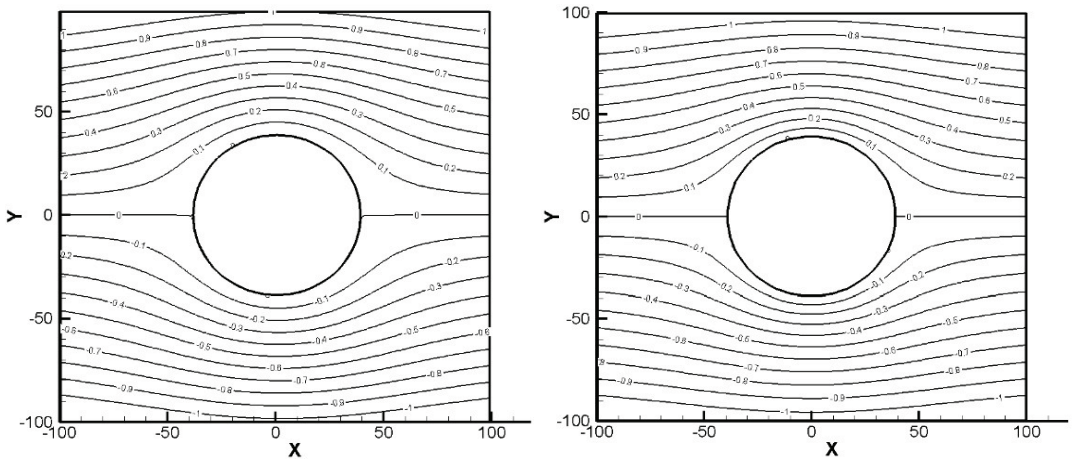

Figure 7: Normalized stream function contours for the flow around a circular cylinder: LBM (left), Analytical (right).

pass through the same point (the doublet center). As mentioned earlier this is due to the fact that the fluid in the LBM is a real fluid with finite viscosity. This viscosity creates a velocity gradient so it prevents the coexistence of different values of the stream function at the same point like in the case of the potential flow. This also causes the stream function contours to take non-circular shapes.

4.5 Flow around a circular cylinder

The flow around a circular cylinder is modeled by placing a doublet of a given strength in a uniform velocity flow field. The flow around a circular cylinder of 78 Lattice Units diameter is shown in Fig. 7 for a doublet of strength $\Gamma = 0.02$ based on $\rho_s = \rho$ (Case I) combined with a uniform velocity of $u_{\text{lattice}} = 0.002$.

5 Discussion and Conclusions

From the results of the numerical simulations, it is clear that the proposed lattice Boltzmann equation is efficient in modeling a point source, sink and doublet of any strength either alone or combined with other flow features like the uniform velocity flow field. This demonstrates the technique's ability to model different elementary flow features.

A lattice Boltzmann method for modeling elementary flows is proposed. The added source term has point symmetry for a point source or sink, while it has line symmetry for the doublet. This allows it to be used along symmetry planes which can result in the reduction of the computational effort. The source or doublet strength can be thought of as a pressure term. Its value can be adjusted to achieve a certain pressure or a pressure difference at a specific point in the domain. It can be used at any place inside the domain with no restrictions, and it does not cause any singularity

problems in the accuracy or the convergence rate of the numerical scheme.

The method has many advantages and can be easily incorporated into any problem. The model can be easily incorporated in the framework of the recent advances in the field of potential flows for viscous fluids. The extension to the three dimensional case is straight forward. The results for some benchmark problems are compared to the analytical solution and excellent agreement between results is found.

References

[1] B. DONG, Y. YAN, W. WAN AND Y. SONG, *Lattice Boltzmann simulation of viscous fingering phenomenon of immiscible fluids displacement in a channel*, Comput. Fluids., 39 (2010), pp. 768–779.

[2] G. GEORGIOU, L. OLSON, W. SCHULTZ AND S. SAGAN, *A singular finite element for stokes flow: the stick-slip problem*, Int. J. Numer. Meth. Fl., 9 (1989), pp. 1353–1367.

[3] H. HUANG AND X. LU, *Theoretical and numerical study of axisymmetric lattice Boltzmann models*, Phys. Rev. E., 80 (2009), 016701.

[4] H. HOLSTEIN AND D. PADDON, *A singular finite difference treatment of re-entrant corner flow, part 1: Newtonian fluids*, J. Non-Newton. Fluid., 8 (1981), pp. 81–93.

[5] D. JOSEPH, T. FUNADA AND J. WANG, Potential Flows of Viscous and Viscoelastic Fluids, Cambridge University Press, New York, 2008.

[6] I. KARLIN, *Exact summation of the Chapman-Enskog expansion from moment equations*, J. Phys. A–Math. Gen., 33 (2000), pp. 8037–8046.

[7] R. LI, T. TANG AND P. ZHANG, *A moving mesh finite element algorithm for singular problems in two and three space dimensions*, J. Comput. Phys., 177 (2002), pp. 365–393.

[8] R. MEI, W. SHYY, D. YU AND L. LUO, *Lattice Boltzmann method for 3-D flows with curved boundary*, J. Comput. Phys., 161 (2000), pp. 680–699.

[9] H. MOFFATT, *Viscous and resistive eddies near a sharp corner*, J. Fluid. Mech., 18 (1964), pp. 1–18.

[10] A. MOHAMAD, Applied Lattice Boltzmann Method for Transport Phenomena, Momentum, Heat and Mass Transfer, SURE Print, Calgary, 2007.

[11] B. MUNSON, D. YOUNG AND T. OKIISHI, Fundamentals of Fluid Mechanics, Fifth Ed., JohnWiley & Sons, Inc., New Jersey, 2005.

[12] R. NOURGALIEV, T. DINH, T. THEOFANOUS AND D. JOSEPH, *The lattice Boltzmann equation method: theoretical interpretation, numerics and implications*, Int. J. Multiphas. Flow., 29 (2003), pp. 117–169.

[13] R. PANTON, Incompressible Flow, Third Ed., JohnWiley & Sons, Inc., New Jersey, 2005.

[14] X. SHAN AND H. CHEN, *Lattice Boltzmann model for simulation flow with multiple phases and components*, Phys. Rev. E., 47 (1993), pp. 1815–1819.

[15] S. SUCCI, The Lattice Boltzmann Equation for Fluid Dynamics and Beyond, Oxford University Press, New York, 2001.

[16] M. SUKOP AND D. THORNE, Lattice Boltzmann Modeling: An Introduction for Geoscientists and Engineers, First Ed, Springer, New York, 2007.

[17] J. WANG AND D. JOSEPH, *Purely irrotational theories of the effect of the viscosity on the decay of free gravity waves*, J. Fluid. Mech., 559 (2006), pp. 461–472.

[18] J. WANG AND D. JOSEPH, *Pressure corrections for the effects of viscosity on the irrotational flow outside Prandtls boundary layer*, J. Fluid. Mech., 557 (2006), pp. 145–165.

[19] J. WANG AND D. JOSEPH, *Boundary layer analysis for effects of viscosity of the irrotational flow on the flow induced by a rapidly rotating cylinder in a uniform stream*, J. Fluid. Mech., 557 (2006), pp. 167–190.
[20] D. WOLF-GLADROW, Lattice-Gas Cellular automata and Lattice Boltzmann Models: an Introduction, Lecture Notes in Mathematics, No. 1725, Springer, New York, 2000.
[21] P. YUAN AND L. SCHAEFER, *Equations of state in a lattice Boltzmann model*, Phys. Fluids., 18 (2006), 042101.
[22] L. ZHENG, B. SHI, Z. GUO AND C. ZHENG, *Lattice Boltzmann equation for axisymmetric thermal flows*, Comput. Fluids., 39 (2010), pp. 945–952.
[23] J. ZHOU, Lattice Boltzmann Methods for Shallow Water Flows, Springer, New York, 2004.
[24] J. ZHOU, *Axisymmetric lattice Boltzmann method*, Phys. Rev. E., 78 (2008), 036701.
[25] Q. ZOU AND X. HE, *On pressure and velocity boundary conditions for the lattice Boltzmann BGK model*, Phys. Fluids., 9 (1997), pp. 1591–1598.